Design of Modular BMS and Real-Time Practical Implementation for Electric Motorcycle Application

Henar Mike O. Canilang, *Graduate Student Member, IEEE*, Angela C. Caliwag, and Wansu Lim, *Member, IEEE*

***Abstract*—Battery management systems (BMSs) are widely used in different battery applications to maximize the system operating efficiency. Due to different applications of BMS, different topologies are developed and used for implementation. In this letter, we propose a modular BMS circuit for electric motorcycles battery voltage applications and present a BMS platform for testing. We conduct a real-time evaluation of the BMS in the designed BMS platform considering a varying total input load voltage ranging from 51.2–67.2 V. The real-time evaluation is conducted using four local modules and one central module. The results are verified using the BMS platform designed for this specific BMS. The BMS voltage measurement accuracy is evaluated. Actual input load voltage values are used to verify the voltage values measured by the BMS, and significantly high accuracy is achieved with a mean RMSE of 0.0018895. In terms of relative error, a mean value of 0.03575 is achieved for the four-cell modular BMS application.**

***Index Terms*—Battery management system (BMS), BMS efficiency, modular topology, motorcycle application, real-time simulation.**

I. Introduction

BATTERY management systems (BMSs) monitor, control, and protect battery cells to address inconsistencies within them that lead to performance instability, such as early ageing effects or cell degradation [1]. BMS topologies can be classified into three categories: 1) centralized, 2) distributed, and 3) modular. Among these, the modular topology is proven to be the most efficient. In a modular topology, each battery module is monitored, controlled and protected by a local management unit (LMU). Moreover, the LMUs are monitored and controlled by a central management unit (CMU).

Several researchers have attempted to improve BMSs with a modular topology. In [2], a hybrid balancing approach consisting of passive and active balancing was presented for a BMS with a modular topology. Specifically, this brief proposed module-level active balancing and cell-level passive balancing using a shared serial communication bus. However, this communication interface requires data transfer through modules going to the central MCU, which is inefficient in terms of module fault detection. In [3], a cascaded modular battery system was presented. Compared with existing approaches, it eliminates the need for excessive balancing of circuits and maximizes the overall performance of each module. Furthermore, in [4], a modular active charge balancing and control scheme architecture was proposed to increase the overall system performance and reduce the overall system complexity. In [5], a modular BMS for high power battery packs for motorsport applications was presented wherein only one LMU and one CMU were employed, namely, power and control boards, respectively. Several studies have focused on improving BMSs with a modular topology. However, most of them have failed to consider the real-time practical applications of these systems.

In this brief, we propose a design of modular BMS for lithium-ion battery and its application to real-time practical implementation. The main objective of this brief is to design and implement both the software and hardware of a BMS with a modular topology that is suitable for practical applications, for example, in an electric motorcycle battery voltage range. The contributions of this brief are as follows: 1) design and implementation of a modular BMS circuit, 2) design and implementation of a modular BMS platform, and 3) integration of the designed modular BMS circuit to a BMS simulation platform for the real-time practical application.

II. Proposed Modular BMS

The proposed modular BMS consists of four LMUs and one CMU. The LMUs monitor, control, and protect all the lithium-ion cells in each module. In contrast, the CMU receives data from each LMU for lithium-ion battery pack monitoring, control, and protection.

A. Modular BMS Circuit

Fig. 1 illustrates the proposed modular design approach for BMS applications. The lithium-ion battery pack [Fig. 1 (a)] has a safe operating voltage range of 51.2–67.2 V with a nominal voltage of 57.6 V and a 16s1p configuration. It consists of four modules, each with a 4s1p configuration. Moreover, each module has a safe operating voltage range of 12.8–16.8 V with a nominal voltage of 14.4 V. Each module consists of

Manuscript received May 29, 2021; accepted June 28, 2021. Date of publication July 1, 2021; date of current version January 31, 2022. This work was supported by the Ministry of Small and Medium Enterprises (SMEs) and Start-Ups, South Korea, under Grant S2829065 and Grant S3010704, and in part by the National Research Foundation of Korea under Grant 2020R1A4A101777511 and Grant 2021R1I1A3056900. This brief was recommended by Associate Editor Z. Galias. *(Corresponding author: Wansu Lim.)*

The authors are with the Department of Aeronautics, Mechanical and Electronic Convergence Engineering, Kumoh National Institute of Technology, Gumi 39177, South Korea (e-mail: wansu.lim@kumoh.ac.kr).

Color versions of one or more figures in this article are available at https://doi.org/10.1109/TCSII.2021.3093937.

Digital Object Identifier 10.1109/TCSII.2021.3093937

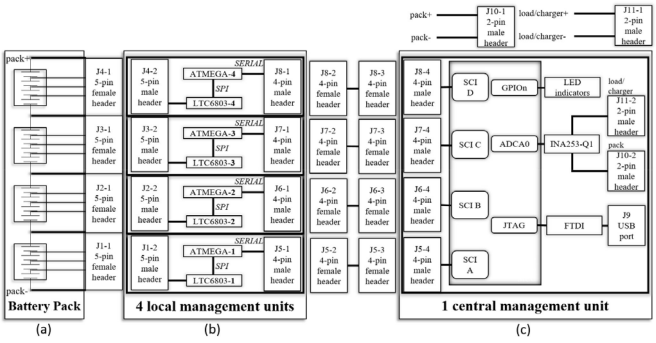

Fig. 1. Overview of the battery management system (BMS).

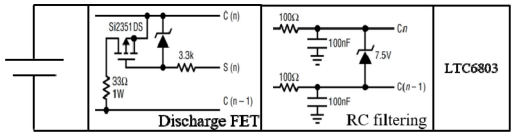

Fig. 2. Local management unit: voltage monitoring circuit.

four lithium-ion cells, in which each cell has a safe operating voltage range of 3.2–4.2 V with a nominal voltage of 3.6 V [6]–[7]. Modules labeled in Fig. 1 (b) and Fig. 1 (c) represent the LMUs and the CMU, respectively.

In each module, all cells are monitored by an LMU. Each LMU has two main components namely: 1) an LTC6803IG battery monitoring IC and a high-performance low-power local MCU 2) ATMEGA328P IC. A detailed block diagram of the voltage monitoring circuit of LMU is presented in Fig. 2. In particular, a set of two different circuits, namely, a discharge FET circuit and a RC filtering circuit, are connected to each cell. The discharge FET is used to discharge cells with a higher voltage than that of other cells. It consists of a high impedance discrete P-MOSFET device and a discharge resistor. On the other hand, the RC filtering circuit filters out the transient voltages and reduces the error in Analog-to-Digital converter (ADC) conversions. For this application, a 16 kHz RC filtering is optimal for the current BMS design which is consist of a 100Ω resistance and a 0.1μF capacitance. The designated resistance value is 100Ω considering the overall operating temperature of the battery management system and its operation power loss due to heat dissipation. This modular BMS' complete battery monitoring IC implements a sampling system for execution of the ADC conversion. An average of 0.5ms conversion window is yielded provided that all signals are distinguishable, adhering to the sigma-delta modulator rate of 512 kHz. An internal 8 parts-per-million per degree Celsius (ppm/°C) voltage reference combined with the ADC give the LTC6803 its outstanding measurement accuracy. The sigma-delta ADC in this design outputs a 12-bit code with an offset of 0x200 (512 decimal). The input voltage is represented as

$$V_{INPUT} = (D_{OUT} - 512) \times V_{LSB}. \quad (1)$$

D_{OUT} is digital output in a form of decimal integer and V_{LSB} is the least significant bit voltage with a value of 1.5mV. The RC filtering circuit is consists of a series resistor and a shunt capacitor with 30db attenuation.

The LMU is isolated; it independently performs cell management and collects the overall cell operational parameter data. The connected cells supplies power to the LMU. In particular, a low voltage to low voltage DC/DC converter IC PLMR50410XDBVR is used to convert the terminal load voltage of the cells in a module to produce the operating voltage required to power the LMU. Moreover, to isolate the LMU, the ADUM2211TRIZ digital isolator is used to address varying system voltage. This enables voltage conversion on the isolation barrier for the LMU to CMU serial communication channels. This LMU design approach solves the data traffic problem, also known as bottleneck, in LMU to CMU communication. Furthermore, the local microcontroller in each LMU monitors the cell voltage and computes the module voltage as the sum of all cell voltages. Additionally, an LT6004IMS8 IC is used for each LMU as a buffer circuit for temperature monitoring. Finally, the LMUs send the voltage and temperature data of the corresponding module to the CMU. Its low power consumption leads to each cell's life and performance maximization. A central management unit manages all the cell parameters. The central MCU converts the digital signals received from LMUs to their equivalent current values for monitoring. Moreover, it monitors the battery pack voltage, current and temperature. Specifically, the CMU consists of two main components: 1) current measurement IC (INA253-Q1) and 2) central MCU (F28379D C2000). The current measurement IC is connected between the battery pack and the charger/load.

B. Modular BMS Platform

In this BMS testing, the MATLAB SIMULINK platform is used to upload code and deploy algorithms on the LMU and CMU hardware. Codes and algorithms are required by the LMUs and the CMU to perform the following BMS testing tasks: For LMUs, 1) cell voltage measurement, 2) module temperature measurement, and 3) cell balancing; whereas the CMU requires them to monitor the module voltage and temperature. The algorithms necessary to perform these functions were built using SIMULINK blocks. The following steps were performed to integrate the hardware and software: 1) import C++ libraries for the MCU, 2) build the designed algorithm in SIMULINK, 3) test it in the external mode, and finally, 4) deploy it to the hardware. First, the necessary C++ libraries were imported. Specifically, the MCUs used in this brief (ATMEGA and C2000) were provided with C++ libraries that could be imported to MATLAB SIMULINK using the S-function builder block, which enables the integration of C/C++ language to the SIMULINK blocks. Second, using the SIMULINK blocks, the algorithm design was built. Subsequently, the algorithm was tested in the external mode, which performs real-time execution of algorithms on the MCU. In particular, it enables real-time signal acquisition and parameter tuning, which are needed when debugging the algorithms. Finally, the testing algorithm was uploaded and deployed to the hardware.

After designing both hardware and software, the software is integrated to the hardware by uploading the code to the

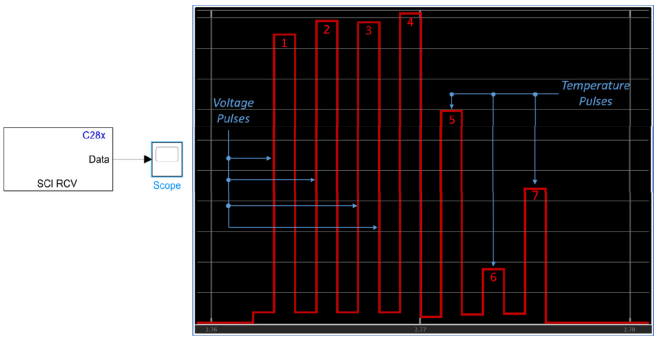

Fig. 3. Central MCU (a) sample SCI receive block and (b) scope output.

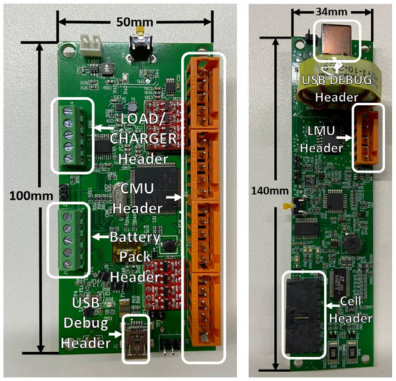

Fig. 4. Actual photograph of the proposed BMS. (a) the CMU and (b) LMU.

TABLE I
AVERAGE RMSE (%) OF EACH LMU MODULE

LMU 1	Cell 1	Cell 2	Cell 3	Cell 4	Simulation time (s)
Actual Voltage (V)	3.2V	3.6V	3.7V	4.2V	
Cell 1 (V)	3.200	3.606	3.7001	4.2022	1800s
Cell 2 (V)	3.201	3.603	3.7005	4.2055	1800s
Cell 3 (V)	3.201	3.599	3.7011	4.2025	1800s
Cell 4 (V)	3.201	3.600	3.7002	4.2011	1800s
RMSE (%)	0.00057	0.003	0.0006	0.0033	-
LMU 2	Cell 1	Cell 2	Cell 3	Cell 4	Simulation time (s)
Actual Voltage (V)	3.2V	3.6V	3.7V	4.2V	
Cell 1 (V)	3.202	3.600	3.702	4.200	1800s
Cell 2 (V)	3.201	3.600	3.701	4.202	1800s
Cell 3 (V)	3.199	3.600	3.701	4.200	1800s
Cell 4 (V)	3.200	3.600	3.701	4.200	1800s
RMSE (%)	0.001	0.0001	0.001	0.001	-
LMU 3	Cell 1	Cell 2	Cell 3	Cell 4	Simulation time (s)
Actual Voltage (V)	3.2V	3.6V	3.7V	4.2V	
Cell 1 (V)	3.200	3.601	3.703	4.2001	1800s
Cell 2 (V)	3.201	3.601	3.7002	4.202	1800s
Cell 3 (V)	3.200	3.600	3.7	4.200	1800s
Cell 4 (V)	3.206	3.601	3.709	4.201	1800s
RMSE (%)	0.003	0.001	0.0049	0.0008	-
LMU 4	Cell 1	Cell 2	Cell 3	Cell 4	Simulation time (s)
Actual Voltage (V)	3.2V	3.6V	3.7V	4.2V	
Cell 1 (V)	3.200	3.602	3.703	4.200	1800s
Cell 2 (V)	3.201	3.600	3.700	4.202	1800s
Cell 3 (V)	3.2002	3.600	3.6998	4.2002	1800s
Cell 4 (V)	3.2005	3.607	3.709	4.201	1800s
RMSE (%)	0.00076	0.003	0.0048	0.0014	-

microcontrollers of the management units (LMUs and CMU). The CMU received the cell voltages and temperature from the LMUs via the Serial Communication Interface. An example of a receiving block in the SIMULINK-modelled algorithm and its output are depicted in Figs. 3 (a) and (b), respectively. The Serial Communication Interface Receiver (SCIRCV) block in Fig. 3 (a) receives the voltage and temperature from the LMU. The output of the SCIRCV block [Fig. 3 (a)] is sent to the Scope block, which enables the visualization of signals by plotting/graphing them. This plot is presented in Fig. 3 (b). The central MCU receives data at a definite interval. A zoom in of the scope shows 7 pulses. This represents 1) 4 cell voltages and 2) 3 temperature readings.

C. Actual Modular BMS

The actual PCB of the BMS circuit is presented in Fig. 4. Each LMU has a 140 x 34 mm board size with only 2 layers. Moreover, it had three headers that provided connection to: 1) each cell in the battery module, 2) CMU, and 3) the USB debug header. On the other hand, the CMU had a 100 x 50 mm board size with 2 layers. Specifically, it had four types of headers that provided connection to: 1) the LMUs, 2) battery pack, 3) load/charger, and 4) the USB debug header. Both boards had the following specifications: FR4 material, HASL lead free surface finish, 1.6 mm finish thickness, and 0.028kg copper thickness.

III. RESULTS AND DISCUSSIONS

In this brief, we performed a real-time practical performance analysis of the implemented modular BMS to test the circuit advantage in terms of voltage measurement accuracy. The average total simulation time for BMS is 1800s. The designed modular BMS circuit was implemented and deployed to the designed BMS platform considering the voltage range for electric motorcycle applications. The LMU cell header is supplied by a power supply with varying terminal voltage values for monitoring the voltage measurement accuracy. Precise voltage measurement accuracy is a key element to battery management design. Any errors in battery cells' voltage measurement directly affects the remaining useful life of the cell. This shows how critical cell voltage measurement is to BMS applications such as for cell balancing, state-of-charge, state-of-health, prognostics, and other BMS algorithms. Each LMUs connected to CMU module is simulated independently. Cross-module performance analysis of each LMU module connected to CMU is performed for further verification of results. A faulty module is removed from the modular system and is tested for each LMU modules to show an adaptive advantage of a modular BMS is in terms of overall operation even when a LMU is at fault.

Each LMU module was initially supplied with the minimum terminal voltage value of 12.8V, which meant that each cell had a load of 3.2V. The terminal voltage was then raised to 14.4V which is the nominal voltage which gives each cell

TABLE II
LMU VOLTAGE MEASUREMENT CROSS-PERFORMANCE ANALYSIS

Actual Voltage Input : 14.4V (Nominal)				**1 Faulty LMU**								
Fault	LMU 1			LMU 2			LMU 3			LMU 4		
Active Module	LMU 2	LMU 3	LMU 4	LMU 1	LMU 3	LMU 4	LMU 1	LMU 2	LMU 4	LMU 1	LMU 2	LMU 3
Average (V)	3.602	3.6001	3.601	3.602	3.6	3.602	3.603	3.601	3.603	3.603	3.602	3.604
RMSE	0.002	0.002	0.002	0.003	0.002	0.003	0.003	0.003	0.003	0.005	0.003	0.004
2 Faulty LMUs												
Fault	LMU 1 and LMU 2			LMU 1 and LMU 3			LMU 1 and LMU 4			LMU 2 and LMU 4		
Active Module	LMU 3	LMU 4		LMU 2	LMU 4		LMU 2	LMU 3		LMU 1	LMU 3	
Average (V)	3.604	3.605		3.602	3.604		3.603	3.598		3.603	3.602	
RMSE	0.004	0.0056		0.003	0.0045		0.003	0.005		0.004	0.002	
3 Faulty LMUs												
Fault	LMU 1 , LMU 2 and LMU 3			LMU 1 , LMU 3 and LMU 4			LMU 1 , LMU 2 and LMU 4			LMU 2 , LMU 3 and LMU 4		
Active Module	LMU 4			LMU 2			LMU 3			LMU 1		
Average (V)	3.603			3.602			3.603			3.602		
RMSE	0.003			0.003			0.003			0.002		

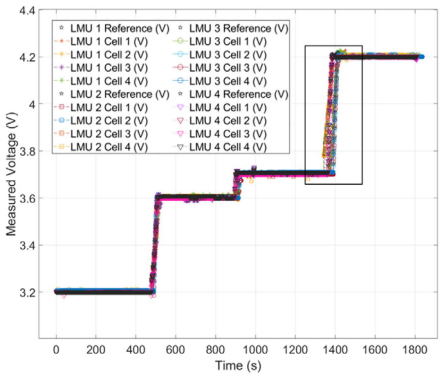

Fig. 5. BMS platform simulation results (actual voltage vs measured voltage).

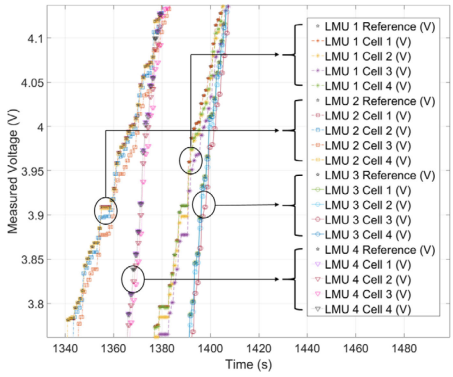

Fig. 6. LMUs 1-4 Voltage Measurement (3.7V to 4.2V transition).

of the LMU 3.6V. The voltage between the minimum and maximum value was also simulated which given a value of 14.8V while the last simulation is for the maximum voltage of 16.8V for each LMU. Overall, the modular BMS's total simulated terminal voltage values for 1 CMU and four LMUs are 51.2V, 57.6V, 59.2V and 67.2V. The 51.2V to 67.2V adheres to our target application which is for electric motorcycles. Cells 1-4 of LMUs 1-4 has yielded an accurate result. Table I presents the actual voltage applied to the modular BMS and LMUs 1-4 average voltage measurement for each cells with respect to the simulation time. The RMSE voltage measured for each cells 1-4 in LMUs 1-4 module is 0.0013, 0.0018, 0.00282 and 0.001625 respectively. This yields a mean RMSE of 0.0018895. The voltages of each LMUs' cells 1, 2, 3, and 4 are stable throughout the test, as plotted in Fig. 5. The average temperature of each cells in the LMU is 29.61℃, as measured with respect to simulation time. This adheres to the lithium-ion battery operating temperature value of 10°C to +55°C. On the other hand, the average measured current of the modular BMS is 8mA. This brief focuses on voltage measurement accuracy.

Fig. 5 plots the actual voltage against the measured voltage results of the modular BMS deployed in the BMS simulation platform. The deployment of the modular BMS circuit to the simulation platform shows the successful integration of the

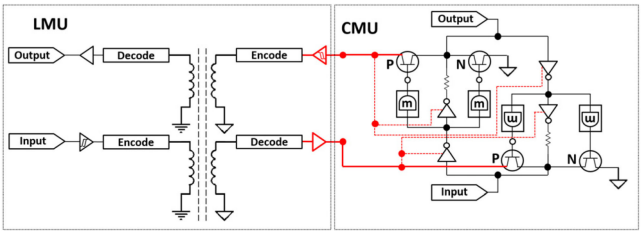

Fig. 7. LMU to CMU communication channel circuit diagram.

BMS hardware to the simulation platform for real-time practical applications. The rectangular box in Fig. 5 highlights the transition from 3.7V – 4.2V cell voltage measurement. Fig. 6 shows a magnified view of LMUs 1-4 voltage measurement for each cell at 1340s to 1415s simulation time. The measured voltage vs the actual voltage shows a stable relation in each cells which indicates high voltage measurement accuracy. Table II presents this modular BMS' cross-performance analysis. This table shows an advantage of this BMS by simulating with faulty LMU modules. To enable simulation with faulty modules, the communication channels of each LMUs to CMU is isolated as presented in Fig. 7.

The circuit branch highlighted in red is the common node for the LMU to CMU communication which is separated by the LMU isolation barrier and the CMU bidirectional translator. When a fault occurs, this node of the LMU to CMU

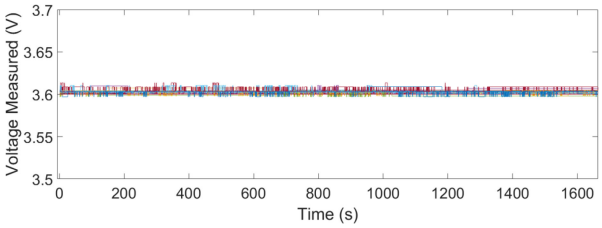

Fig. 8. Cross-performance analysis measured voltage.

TABLE III
AVERAGE RELATIVE ERROR COMPARISON OF THE BMS VOLTAGE MONITORING

Relative Error (%)	[8]	[9]	[10]	Proposed Method
Cell 1	0.028	0.55	0.08	0.028
Cell 2	0.056	0.81	0.12	0.034
Cell 3	0	0.27	0.093	0.051
Cell 4	0.139	-	0.23	0.030
Average	0.058	0.54	0.1308	0.03575

channel prevents further system damage. This approach keeps the BMS performance stable despite having faulty modules.

For this simulation analysis, the 3.6V nominal voltage for each lithium-ion cells was used as the reference voltage. This gives a total 14.4V which is the nominal voltage for each LMU.

Fig. 8 shows the measured voltage for the modular BMS' cross performance analysis presented in Table II. These results concretely proves that our modular BMS design adheres to the ISO 26262 standards known as the "Road vehicles – Functional Safety". The graph shows the stable voltage measurement of each LMU despite faults applied in the simulation. It is comparable in both Tables I and II that there is a negligible difference between the RMSE of voltage measured by each cells in a module. The mean RMSE yielded by this cross performance analysis is 0.0032125. Table III presents the relative error comparison of studies that presented BMS voltage measurements. Most studies presented average values of actual voltage vs measured voltage for cells 1-4, which were used for verification. For verification of this brief, we performed real-time testing of the modular BMS in the designed platform for an average of 1800 seconds for electric motorcycle battery voltage application. From this real-time implementation, we acquired the average cells 1-4 voltage measurements of each LMUs for varying voltage from 3.2 – 4.2V respectively, as presented in Table II. The relative error of the actual voltage vs measured voltage is 0.028%, 0.034%, 0.051%, and 0.030% for each LMUs' Cells 1 – 4, respectively. The average relative error of the designed modular BMS for voltage monitoring is 0.03575% which is lower compared with implementations of [8]–[10]. These results indicated that our work has outperformed other methods proposed by other studies.

As the design progressed, system simulations were conducted to verify sub-circuit efficiency such as for the LMU DC-DC converter. The result showed a 92.74% efficiency. This efficiency has a directly proportional relationship to the overall efficiency of the designed modular BMS since LMU draws power from each connected cells.

IV. CONCLUSION

In this letter, we proposed the design of a modular BMS circuit for lithium-ion battery and its implementation in a real-time BMS platform. The BMS platform is capable of real-time signal acquisition and parameter tuning which a must for practical implementation. The real-time practical implementation for electric motorcycle voltage range application is presented in this brief having a battery voltage range of 51.2–67.2 V. Furthermore, we verified the integration of the circuit and the platform for real-time application. By comparing the actual measured voltage with the input load voltage, a high-efficiency BMS circuit structure was realized. A mean RMSE of 0.0018895 for each LMUs 4 cells was observed. The obtained results indicate strong potential for the implementation of the proposed modular BMS structure.

Part of our future works in the current modular BMS design is to implement 12s1p per LMU to handle higher voltage applications to maximize the capability of the battery monitoring IC.

REFERENCES

[1] A. Farjah and T. Ghanbari, "Early ageing detection of battery cells in battery management system," *Electron. Lett.*, vol. 56, no. 12, pp. 616–619, 2020.

[2] F. Zhang, M. M. U. Rehman, R. Zane, and D. Maksimović, "Hybrid balancing in a modular battery management system for electric-drive vehicles," in *Proc. IEEE Energy Convers. Congr. Exposit. (ECCE)*, Oct. 2017, pp. 578–583.

[3] A. M. Fares, C. Klumpner, and M. Sumner, "Optimising the structure of a cascaded modular battery system for enhancing the performance of battery packs," *J. Eng.*, vol. 2019, no. 17, pp. 3862–3866, Jun. 2019.

[4] S. Narayanaswamy, M. Kauer, S. Steinhorst, M. Lukasiewycz, and S. Chakraborty, "Modular active charge balancing for scalable battery packs," *IEEE Trans. Very Large Scale Integr. (VLSI) Syst.*, vol. 25, no. 3, pp. 974–987, Mar. 2017.

[5] U. Abronzini *et al.*, "Optimal modular BMS for high performances NMC battery pack," in *Proc. IEEE Int. Conf. Elect. Syst. Aircraft Railway Ship Propulsion Road Veh. Int. Transp. Electrif. Conf. (ESARS-ITEC)*, Nottingham, U.K., Nov. 2018, pp. 1–6.

[6] S. Wang and P. K. T. Mok, "An 18-nA ultra-low-current resistor-less bandgap reference for 2.8 V–4.5 V high voltage supply li-ion-battery-based LSIs," *IEEE Trans. Circuits Syst. II, Exp. Briefs*, vol. 67, no. 11, pp. 2382–2386, Nov. 2020.

[7] Y. Li, M. John, Y. Ramadass, and S. R. Sanders, "AC-coupled stacked dual-active-bridge DC–DC converter for integrated lithium-ion battery power delivery," *IEEE J. Solid-State Circuits*, vol. 54, no. 3, pp. 733–744, Mar. 2019.

[8] Y. Xu, S. Jiang, and T. X. Zhang, "Research and design of lithium battery management system for electric bicycle based on Internet of Things technology," in *Proc. Chin. Autom. Congr. (CAC)*, Hangzhou, China, Nov. 2019, pp. 1121–1125.

[9] F. Zhu, G. Liu, C. Tao, K. Wang, and K. Jiang, "Battery management system for Li-ion battery," *J. Eng.*, vol. 2017, no. 13, pp. 1437–1440, Jan. 2017.

[10] T. Yue, L. Wu, X. Zhang, and G. Tian, "High-precision voltage measurement IP core for battery management SoC of electric vehicles," in *Proc. 12th IEEE Int. Conf. Solid-State Integr. Circuit Technol. (ICSICT)*, Guilin, China, Oct. 2014, pp. 1–3.